

# Potassium Abundances in Red Giants of Mildly to Very Metal-Poor Globular Clusters \* †

Yoichi TAKEDA,<sup>1,2</sup> Hiroyuki KANEKO,<sup>2</sup> Naoko MATSUMOTO,<sup>2</sup>  
Shoichi OSHINO,<sup>2</sup> Hiroko ITO,<sup>2</sup> and Takatoshi SHIBUYA<sup>2</sup>

<sup>1</sup>National Astronomical Observatory, 2-21-1 Osawa, Mitaka, Tokyo 181-8588  
takeda.yoichi@nao.ac.jp

<sup>2</sup>The Graduate University for Advanced Studies, 2-21-1 Osawa, Mitaka, Tokyo 181-8588  
kaneko-h@nro.nao.ac.jp, naoko.matsumoto@nao.ac.jp, shoichi.oshino@nao.ac.jp,  
hiroko.ito@nao.ac.jp, takatoshi.shibuya@nao.ac.jp

(Received 2009 January 21; accepted 2009 February 23)

## Abstract

A non-LTE analysis of K I resonance lines at 7664.91 and 7698.97 Å was carried out for 15 red giants belonging to three globular clusters of different metallicity (M 4, M 13, and M 15) along with two reference early-K giants ( $\rho$  Boo and  $\alpha$  Boo), in order to check whether the K abundances are uniform within a cluster and to investigate the behavior of [K/Fe] ratio at the relevant metallicity range of  $-2.5 \lesssim [\text{Fe}/\text{H}] \lesssim -1$ . We confirmed that [K/H] (as well as [Fe/H]) is almost homogeneous within each cluster to a precision of  $\lesssim 0.1$  dex, though dubiously large deviations are exceptionally seen for two peculiar stars showing signs of considerably increased turbulence in the upper atmosphere. The resulting [K/Fe] ratios are mildly supersolar by a few tenths of dex for three clusters, tending to gradually increase from  $\sim +0.1$ – $0.2$  at  $[\text{Fe}/\text{H}] \sim -1$  to  $\sim +0.3$  at  $[\text{Fe}/\text{H}] \sim -2.5$ . This result connects reasonably well with the [K/Fe] trend of disk stars ( $-1 \lesssim [\text{Fe}/\text{H}]$ ) and that of extremely metal-poor stars ( $-4 \lesssim [\text{Fe}/\text{H}] \lesssim -2.5$ ). That is, [K/Fe] appears to continue a gradual increase from  $[\text{Fe}/\text{H}] \sim 0$  toward a lower metallicity regime down to  $[\text{Fe}/\text{H}] \sim -3$ , where a broad maximum of  $[\text{K}/\text{Fe}] \sim +0.3$ – $0.4$  is attained, possibly followed by a slight downturn at  $[\text{Fe}/\text{H}] \lesssim -3$ .

**Key words:** stars: abundances (potassium) — stars: atmospheres — stars: globular clusters (M 4, M 13, M 15) — stars: late-type — stars: spectra

## 1. Introduction

The chemical evolution of potassium (K) in the Galaxy, which can be investigated by examining its photospheric abundances of old metal-poor stars, is still only insufficiently explored and not yet well understood, especially in the metal-poor regime of halo stars. The main reason for this unsatisfactory situation is presumably the difficulty involved with determinations of stellar potassium abundances, for which only two strong K I lines at 7664.91 and 7698.97 Å (hereinafter referred to as 7665 and 7699 lines for brevity) are practically usable. That is, although these resonance lines are so strong as to be measurable even for stars of extremely low metallicity, the following features make the problem comparatively harder to deal with:

— Above all things, they generally suffer an appreciably large non-LTE effect,<sup>1</sup> which depends on the stel-

lar atmospheric parameters as well as the line strength. Actually, since the extent of the (negative) non-LTE correction amounts from a few tenths dex even up to  $\sim 1$  dex, it is requisite to take account of the non-LTE effect in deriving stellar K abundances.

— Besides, they occasionally suffer serious blending with strong absorption lines originated from earth's atmosphere (especially for the 7665 line) because of being located in an unfavorable wavelength region crowded with such telluric lines. Hence, when encountered with such unfortunate cases, one has to recover the pure stellar spectrum by appropriately eliminating the blended telluric spectrum.

The first non-LTE study of K abundances in metal-poor stars was carried out by Takeda et al. (2002a, here-

\* Based on data collected at Subaru Telescope, which is operated by the National Astronomical Observatory of Japan.

† The electronic table E1 will be made available at the PASJ web site upon publication, while it is provisionally placed at (<http://optik2.mtk.nao.ac.jp/~takeda/GCpotassium/>).

<sup>1</sup> While non-LTE line formation of K I 7665/7699 resonance lines specific to the solar atmosphere had begun already in 1980s (see Bruls et al. 1992 and the references therein), non-LTE studies of these K I doublet lines directed to stars other than the Sun gradually appeared in the last decade: Takeda et al. (1996)

carried out a detailed study on the formation of this line in Procyon (along with the Sun). Ivanova and Shimanskiĭ (2000) calculated non-LTE abundance corrections applicable to A–K stars of wide parameter ranges. Similarly, Takeda et al. (2002a) carried out extensive non-LTE calculations on a grid of models and published tables of non-LTE corrections applicable to F–G–K dwarfs through supergiants. Recently, Zhang et al. (2006a) performed a careful non-LTE investigation of solar potassium lines with a special attention to clarifying the important atomic parameter of neutral hydrogen collision cross section, which they further applied to determinations of K abundances for metal-poor stars (Zhang & Zhao 2005, Zhang et al. 2006b).

inafter referred to as Paper I). They showed that  $[K/Fe]$  values for the main-sequence stars in the galactic disk ( $-1 \lesssim [Fe/H] \lesssim 0$ ) tend to show a rather tight relation of steadily increasing with a decrease of metallicity (such as like the trend of  $\alpha$ -group elements). This was actually a reconfirmation of the results of Chen et al.'s (2000) LTE analysis, despite the significant non-LTE corrections of  $\sim -0.5$  dex, because the corrections turned out to act similarly on the Sun and these disk dwarfs (i.e.,  $[K/H]$ , the differential stellar potassium abundance relative to the Sun, was eventually not much affected). Such an  $\alpha$ -like trend of  $[K/Fe]$  for disk stars was also confirmed by Zhang et al. (2006b).

Unfortunately, the situation becomes quite uncertain when we go into the much lower metallicity regime ( $[Fe/H] \lesssim -1$ ). It was already noticed in Paper I from the non-LTE reanalysis of the published data for several halo stars of  $[Fe/H] \sim -2$  (Gratton & Sneden 1987b) that their  $[K/Fe]$  values widely spread from  $\sim +0.1$  to  $\sim +0.7$  (cf. figure 4a of Paper I; see also figure 8 of Gratton & Sneden 1987a). Zhang and Zhao (2005) also suggested a considerably large diversity of  $[K/Fe]$  (from  $\sim 0$  to  $\sim 1$ ) for the halo stars of  $-2 \lesssim [Fe/H] \lesssim -1$  they studied (cf. figure 12 therein). On the other hand, however, five halo stars included in Zhang et al.'s (2006) study have nearly the same  $[K/Fe]$  ratios around  $\sim +0.2$  over the range of  $-2 \lesssim [Fe/H] \lesssim -1$  (cf. figure 5 therein). Besides, Cayrel et al. (2004) obtained in their extensive study of extremely metal-poor stars ( $-4 \lesssim [Fe/H] \lesssim -2.5$ ) that  $[K/Fe]$  shows a slightly supersolar trend ( $\sim +0.1$ – $0.2$ ) decreasing toward a very low metallicity with a fairly small scatter (cf. figure 9 therein). Thus, at present, we know little about how the  $[K/Fe]$  ratio actually behaves itself at  $[Fe/H] \lesssim -1$ : Tight trend? Large diversity? Does it smoothly connect to the  $\alpha$ -like clear tendency seen in disk stars at  $[Fe/H] \gtrsim -1$ ?

For the purpose of checking the possibility of K abundance diversity in such metal-deficient halo stars, it would be interesting to study stars in globular clusters, for which any trial of potassium abundance determination has never been reported so far to our knowledge. Admittedly, the elemental abundances of old globular cluster stars may not necessarily be the same as those of field halo stars, given that specific abundance peculiarities are known for several elements (e.g., O, Na, Mg, Al) which are presumably due to dredge-up of nuclear-processed product caused by evolution-induced deep mixing. However, since K is considered to be synthesized mainly via the oxygen burning in high-mass stars, whichever the process is explosive or hydrostatic (see, e.g., table 19 in Woosley & Weaver 1995), it is unlikely that the surface K abundance undergoes any appreciable changes during the course of stellar evolution in low-mass stars of globular clusters. Besides, the fact that no star-to-star variation in globular clusters is observed in the abundances of Ca ( $Z = 20$ , near to  $Z = 19$  of K) may also suggest the inertness of K to nuclear processes in the stellar interior, presumably because of the higher Coulomb barrier compared to lighter elements. Therefore, as a reasonable working hypothesis, we may postulate (such as the case for Fe in most clusters)

that (i) the abundance of K was the same in any stars of a given globular cluster when they were born, that (ii) this uniformity has been retained up to now, and that (iii) the surface K abundances of cluster stars may be regarded to be equivalent to field halo stars of similar metallicity. Accordingly, if we could observationally confirm postulation (ii), this would assure the practical validity of (iii), which means that we may directly compare the results of cluster stars with those of other halo stars in general. Or, alternatively, if we found a markedly large diversity of K abundances within a cluster contrary to postulation (ii), we would have to consider a possibility of real star-to-star variation (or cast doubt on the validity of our abundance determination method).

Motivated by this consideration, we decided to conduct a spectroscopic study on the intrinsically bright red-giant stars of three globular clusters (M 4, M 13, and M 15) covering a wide metallicity span (from  $[Fe/H] \sim -2.5$  to  $\sim -1$ ) based on the high-dispersion spectra obtained with Subaru/HDS, in order to determine the abundance of K for each star while taking into account the non-LTE effect, after having established the atmospheric parameters including  $[Fe/H]$ . What we intend to clarify is, as described above, to check the homogeneity of  $[K/H]$  within a cluster [postulation (ii)], and to study the behavior of  $[K/Fe]$  in halo stars based on the results of these globular clusters [postulation (iii)] while comparing with those of other metallicity regime. This is the purpose of this study.

Besides, in connection with the main subject, we carried out a reanalysis of the equivalent-width data of K I 7665 and 7669 lines for  $\sim 30$  extremely metal-poor stars published by Cayrel et al. (2004), in order to establish the  $[K/Fe]$  vs.  $[Fe/H]$  relation at the metallicity range of  $-4 \lesssim [Fe/H] \lesssim -2.5$ . The main motivation is to properly take into account the non-LTE effect, since their treatment in this respect does not appear to be sufficiently valid (i.e., they applied a tentatively assumed correction uniformly to all stars). This reanalysis is separately described in the Appendix.

## 2. Observational Data

Three globular clusters (M 4, M 13, and M 15) were chosen for this study, because (1) they have different metallicities from each other ( $[Fe/H]_{M15} < [Fe/H]_{M13} < [Fe/H]_{M4}$ ), (2) they are located in near or reasonable distance to us (so that red giants of  $V \lesssim 12$  mag exist), and (3) they are comparatively well studied and a number of literature data may be found. Practically, we selected 5 red-giant stars for each cluster satisfying the criterion of  $4100 \text{ K} \lesssim T_{\text{eff}}^{\text{pho}} \lesssim 4300 \text{ K}$  ( $T_{\text{eff}}^{\text{pho}}$  is the effective temperature photometrically evaluated from  $(B - V)_0$  colors; cf. subsection 5.1): L 2406, L 2617, L 3209, L 3624, and L 4511 for M 4; I-13, II-76, III-52, III-59, and III-73 for M 13; K 144, K 341, K 431, K 634, and K 825 for M 15. These targets belong to the brightest-class group in each cluster ( $V \sim 11$ – $12$  mag for M 4,  $V \sim 12$ – $13$  mag for M 13 and M 15). In addition, two

early-K giant stars of near-solar or subsolar metallicity ( $\rho$  Boo and  $\alpha$  Boo) were also included as the standard stars, though they are normal K giants of luminosity class III with  $\log(L/L_\odot) \sim 2$  while all 15 cluster stars are “tip giants” locating on the tip of asymptotic giant branch at  $\log(L/L_\odot) \sim 3$ .

The observations of these 17 stars (along with a rapid rotator Altair as a reference of telluric lines) were carried out on the night of 2008 August 20 (Hawaii Standard Time) by using the High Dispersion Spectrograph (HDS; Noguchi et al. 2002) placed at the Nasmyth platform of the 8.2-m Subaru Telescope, which can record high-dispersion spectra covering a wavelength portion of  $\sim 2600\text{\AA}$  (in the red cross disperser mode) with two CCDs of  $2\text{K} \times 4\text{K}$  pixels at a time. With the slit width set at  $0.''6$  ( $300\ \mu\text{m}$ ) and a binning of  $2 \times 2$  pixels, the resolving power of the obtained spectra is  $R \sim 60000$ . In the standard “Ra” setting, our spectra cover the wavelength region of  $5100\text{--}6400\ \text{\AA}$  (blue CCD) and  $6500\text{--}7800\ \text{\AA}$  (red CCD), which was so chosen as to make use of the yellow–red region of  $\lambda \gtrsim 5000\text{\AA}$  (where the sensitivity of CCD is large and many Fe lines usable for parameter determinations exist) while including the targeted K I 7665/7699 lines amply. The seeing size was  $0.''5\text{--}0.''6$ , and all of the targets could be successfully observed without any significant influence of neighboring stars. The integrated exposure time for each cluster star was from 10 min (= 5 min  $\times 2$ ; for M 4 stars) to 15–20 min (= 7.5–10 min  $\times 2$ ; for M 13 or M 15 stars).

The reduction of the spectra (bias subtraction, flat-fielding, scattered-light subtraction, spectrum extraction, wavelength calibration, continuum normalization) was performed by using the `echelle` package of the software IRAF<sup>2</sup> in a standard manner. The resulting average S/N ratios were around  $\sim 100\text{--}150$  for each of the 15 cluster stars, while much higher values were attained for the bright reference stars;  $\sim 300\text{--}400$  ( $\rho$  Boo),  $\sim 200\text{--}300$  ( $\alpha$  Boo), and  $\sim 600\text{--}700$  (Altair).

### 3. Atmospheric Parameters

The determination of the atmospheric parameters [ $T_{\text{eff}}$  (effective temperature),  $\log g$  (surface gravity),  $v_t$  (microturbulence), and  $[\text{Fe}/\text{H}]$  ( $\equiv A_{\text{Fe}}^{\text{star}} - A_{\text{Fe}}^\odot$ ; differential Fe abundance relative to the Sun, where  $A_{\text{Fe}}^\odot$  is 7.50 in the usual normalization of  $A_{\text{H}} = 12.00$ )] necessary for constructing model atmospheres was implemented by way of the spectroscopic approach using the equivalent widths ( $EW$ s) of Fe I and Fe II lines, which has a merit of establishing these four parameters based only on the same spectrum to be further used for abundance determinations.

Practically, we used the computer program (named TGVIT) developed for this purpose (Takeda et al. 2005; cf. section 2 therein), which is based on the principle

of searching for the most optimum solution in the 3-dimensional ( $T_{\text{eff}}, \log g, v_t$ ) space such that simultaneously satisfying the three requirements: (1)  $\chi_{\text{low}}$ -independence of Fe I abundances (excitation equilibrium, where  $\chi_{\text{low}}$  is the lower excitation potential), (2) equality of the mean abundance derived from Fe I lines and that from Fe II lines (ionization equilibrium), and (3)  $EW$ -independence of the abundances (curve-of-growth matching), as described in Takeda, Ohkubo, and Sadakane (2002b). Since low-gravity K-type giants are specifically involved in this study, we newly computed a grid of data files [covering the parameter ranges of  $3750\text{--}5000\ \text{K}$  in  $T_{\text{eff}}$  (K),  $0.0\text{--}2.5$  in  $\log g$  ( $\text{cm s}^{-2}$ ),  $0.0\text{--}4.0$  in  $v_t$  ( $\text{km s}^{-1}$ ), and  $-2.5$  to  $+0.1$  in  $[\text{Fe}/\text{H}]$  (dex)] to be used in application of TGVIT by interpolation (or extrapolation).

First, we measured the  $EW$ s of available lines by consulting the list of 330 Fe lines (cf. electronic table E1 in Takeda et al. 2005) by using the Gaussian fitting method, where only lines weaker than  $100\ \text{m}\text{\AA}$  were used in order to make sure that errors caused by damping wings/parameters are suppressed to a negligible level. Then, given these  $EW$  data as inputs, the converged solutions of  $T_{\text{eff}}, \log g$ , and  $v_t$  (along with  $A_{\text{Fe}}$  as a product) were established by iteratively running TGVIT (cf. subsection 3.2 in Takeda et al. 2005). The resulting parameter solutions are summarized in table 1, while the detailed  $EW$  data and the Fe abundances corresponding to the final parameters for each star are presented in electronic table E1. The trend of the Fe abundances corresponding to the final solutions is plotted against  $EW$  as well as  $\chi_{\text{low}}$  in figure 1, where we can see that the required conditions are reasonably accomplished.

The internal statistical errors involved with these solutions of  $T_{\text{eff}}, \log g, v_t$ , and  $[\text{Fe}/\text{H}]$ , which were derived by the procedure described in subsection 5.2 of Takeda, Ohkubo, and Sadakane (2002b), turned out to be  $\sim 10\text{--}30\ \text{K}$ ,  $\sim 0.05\text{--}0.1$  dex,  $\sim 0.1\text{--}0.4\ \text{km s}^{-1}$ , and  $\sim 0.03\text{--}0.1$  dex, respectively. We will discuss in subsection 4.1 these spectroscopic parameters in comparison with those derived from the conventional method (i.e., use of photometric colors or evolutionary tracks).

## 4. Analysis of Potassium Lines

### 4.1. $EW$ Measurement

Among our 17 target stars, 5 stars of M 13 were found to be associated with the most unfortunate case. The K I 7699 line could not be measured at all because it happened to fall just on the narrow inter-order gap of HDS (at  $7687\text{--}7694\ \text{\AA}$ ) due to M 13’s large (negative) radial velocity of  $\sim -220$  to  $-230\ \text{km s}^{-1}$ , while the K I 7665 line was seriously blended with the strong telluric  $\text{O}_2$  line at  $7659.3\ \text{\AA}$ . Such a contamination in the K I 7665 region is also seen for the case of two standard stars,  $\alpha$  Boo and (especially)  $\rho$  Boo, which turned out to be influenced by the telluric  $\text{O}_2$  doublet at  $\sim 7664/7665\ \text{\AA}$ . We, therefore, tried to eliminate the effect of telluric lines for these 7 stars by dividing the raw spectra by the spectrum of Altair (rapid rotator) by using the IRAF task `telluric`.

<sup>2</sup> IRAF is distributed by the National Optical Astronomy Observatories, which is operated by the Association of Universities for Research in Astronomy, Inc. under cooperative agreement with the National Science Foundation.

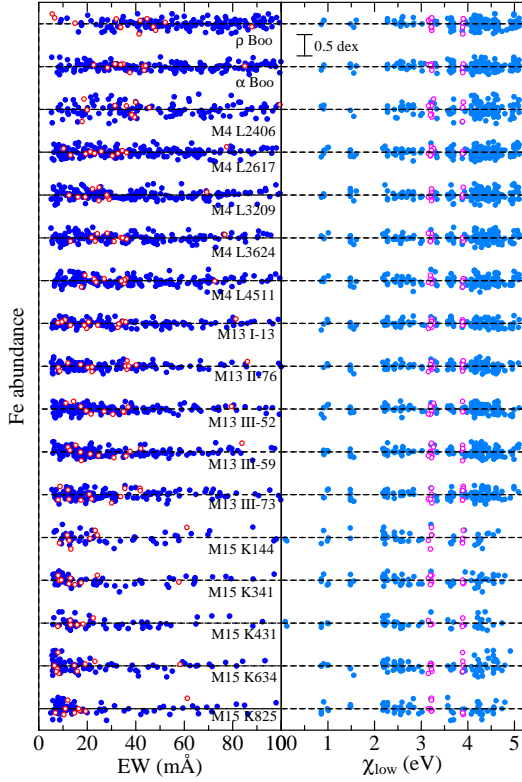


**Fig. 1.** Fe abundance vs. equivalent width relation (left panel) and Fe abundance vs. lower excitation potential relation (right panel) corresponding to the finally established atmospheric parameters of  $T_{\text{eff}}$ ,  $\log g$ , and  $v_t$  for each of the 17 stars. The filled (blue) and open (red) circles correspond to Fe I and Fe II lines, respectively. The results for each star are shown relative to the mean abundance indicated by the horizontal dashed line, and vertically offset by 1.0 relative to the adjacent ones.

The resulting as well as the original spectra are shown in figure 2, where we can see that this elimination surely worked (though not perfectly). Figure 3 displays the spectra used for measurements of  $EW_{7665}$  and  $EW_{7699}$ , which were measured by the Gaussian fitting method as for the case of Fe lines. The finally adopted values of  $EW_{7665}$ <sup>3</sup> and  $EW_{7699}$  are summarized in table 1.

<sup>3</sup> Actually, we had to apply further corrections to  $EW_{7665}$  for five M 13 stars (I-13, II-76, III-52, III-59, and III-73) and  $\rho$  Boo, for which we tried elimination of telluric lines ( $EW_{7665}$  for  $\alpha$  Boo does not need to be corrected, since the important line core was free from contamination). Namely, given that this removal could not be completely done, as can be recognized from the appreciable residual at the position of the redward component of the relevant O<sub>2</sub> doublet (at 7660.4 Å for M 13 stars and at 7665.9 Å for  $\rho$  Boo; see the depression marked with “x” in figure 2), we evaluated its equivalent width ( $\Delta EW_{\text{resid}}$ ) and subtracted from the directly measured  $EW$  as  $EW_{7665}^{\text{adopt}} = EW_{7665}^{\text{raw}} - \Delta EW_{\text{resid}}$  for these six stars, assuming that the residuals of both telluric components are almost the same. The applied  $\Delta EW_{\text{resid}}$  corrections are given in the caption of table 1.

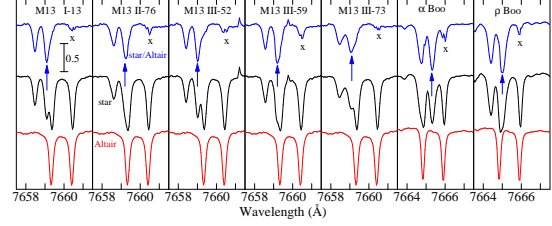


**Fig. 2.** Removal of telluric O<sub>2</sub> lines in the K I 7665 line region for the seven stars significantly suffering this effect. Dividing the raw stellar spectrum (middle, black) by the spectrum of a rapid rotator Altair (bottom, red) results in the final spectrum (upper, blue) where the effect of the blending component is reasonably (even if not completely) eliminated. The residual caused by the imperfect elimination for the redward component of the telluric doublet lines is marked by a cross (x), the strength of which is usable for the correction of  $EW(K \text{ I } 7665)$  similarly affected by the incomplete removal of the blueward component. The position of the K I 7665 line is indicated by an arrow. Each spectrum (normalized with respect to the continuum) is vertically offset by 1.0 relative to the adjacent one. No Doppler correction has been applied to the wavelength scale.

#### 4.2. Abundance Determination

The determination of potassium abundances from the measured  $EW_{7665}$  and  $EW_{7699}$  by taking into account the non-LTE effect was carried out in almost the same manner as in Paper I. As the basic grid of model atmospheres, we used Kurucz’s (1993) ATLAS9 models (corresponding to  $v_t = 2 \text{ km s}^{-1}$ ), which were three-dimensionally interpolated (or extrapolated in special cases of negative  $\log g$ ) with respect to  $T_{\text{eff}}$ ,  $\log g$ , and  $[\text{Fe}/\text{H}]$  to generate the atmospheric model for each star.

The non-LTE statistical-equilibrium calculations were implemented for a grid of 90 models resulting from combinations of three  $T_{\text{eff}}$  values (4000, 4250, 4500 K), five  $\log g$  values (0.0, 0.5, 1.0, 1.5, 2.0), and six  $[\text{Fe}/\text{H}]$  values (−2.5, −2.0, −1.5, −1.0, −0.5, 0.0), so that we can obtain the depth-dependent non-LTE departure coefficients for any star by interpolating (or extrapolating) this grid. See Takeda et al. (1996) for the computational details. We suppressed the effect of neutral-hydrogen collisions to a negligible level by multiplying the classical value based on Drawin’s cross section (cf. Steenbock & Holweger 1984) by a factor of  $10^{-4}$  according to the conclusion of that paper.

The derivation of the K abundance from a given  $EW$  was done as in Paper I with Kurucz’s (1993) WIDTH9 program, which had been considerably modified in various respects (especially to include the effect of departure from LTE). According to Takeda et al. (1996), the van der Waals damping parameter ( $C_6$ ) was increased by applying a correction of  $\Delta \log C_6 = +1.00$  to the conventional Unsöld’s (1955) formula value (corresponding to using  $\Gamma_6 = 2.5\Gamma_6^{\text{Unsöld}}$ ). We adopted the  $\log gf$  values of +0.13 (7665 line) and −0.17 (7699 line), and the radiation damping constant of  $\Gamma_{\text{rad}} = 0.38 \times 10^8 \text{ s}^{-1}$ , which

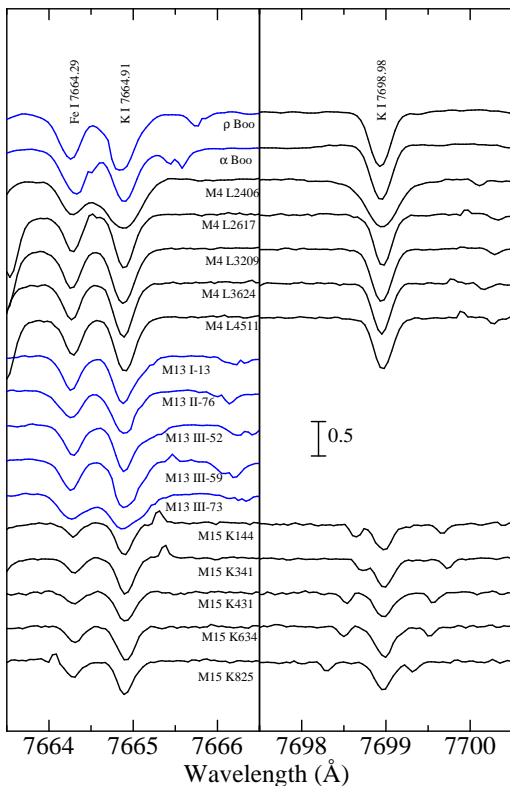


**Fig. 3.** Spectra of 17 stars in the neighborhood of the K I 7665 line (left panel) and the K I 7699 line (right panel). The seven spectra for the two standard stars and five M 13 stars in the left panel (drawn in blue lines) are the ones corrected for the telluric lines (cf. figure 2). Each spectrum (normalized with respect to the continuum) is vertically offset by 0.5 relative to the adjacent one. An appropriate Doppler correction has been applied to each spectrum so that the positions of stellar spectral lines are located at the corresponding laboratory wavelengths.

were taken from Kurucz and Bell’s (1995) compilation.

Actually, we prepared two sets of non-LTE departure coefficients (grid of 90 models) corresponding to two different choices of input K abundances ( $[K/Fe] = 0.0$  and  $[K/Fe] = +0.5$ ), considering that the resulting  $[K/Fe]$  is likely to be encompassed by these two values. And two kinds of non-LTE abundances ( $A_K^{0.0}$  and  $A_K^{0.5}$ ) were obtained for a given  $EW$  for each of the two sets. Then, these  $A_K^{0.0}$  and  $A_K^{0.5}$  were interpolated (or extrapolated) so that the final non-LTE solution ( $A_K$ ) and the used departure coefficient becomes consistent with each other (cf. subsection 4.2 in Takeda & Takada-Hidai 1994). In addition, we also derived the LTE abundance  $A_K^{LTE}$ , from which the non-LTE correction was derived as  $\Delta^{NLTE} \equiv A_K - A_K^{LTE}$ . Finally, the differential K abundance relative to the Sun was computed as  $[K/H] \equiv A_K - 5.12$ , where Anders and Grevesse’s (1989)  $A_{K,\odot}$  value of 5.12 was adopted as the solar potassium abundance (which is also consistent with the result of Takeda et al. 1996). The resulting values of  $[K/H]$  and  $\Delta^{NLTE}$  for each line along with the  $[K/Fe]$  ratio ( $\equiv [K/H] - [Fe/H]$ ;  $[K/H]$  is the average of two lines)

are summarized in table 1. Regarding the typical errors in the K abundances caused by uncertainties in the atmospheric parameters or the damping constant, table 1 in Paper I (especially for the cases of metal-poor K giants such as HD 122563, HD 165195, and HD 221170) may be informative.

## 5. Discussion

### 5.1. Verifying Model Atmosphere Parameters

It may be worth comparing our spectroscopically determined atmospheric parameters with those by another method occasionally used for globular cluster stars; i.e., the photometric  $T_{\text{eff}}^{\text{pho}}$  and evolutionary  $\log g^{\text{evo}}$ , where  $T_{\text{eff}}$  is derived from colors and  $g$  is evaluated from  $L$  (the stellar luminosity estimated from the apparent magnitude and the distance),  $T_{\text{eff}}$ , and  $M$  (the stellar mass often assumed to be  $0.8 M_{\odot}$  for globular cluster giants) by the relation of  $g/g_{\odot} = (M/M_{\odot})(L/L_{\odot})^{-1}(T_{\text{eff}}/T_{\text{eff},\odot})^4$ .

The basic data of  $V$  magnitude and  $B - V$  color were taken from Ivans et al. (1999; M 4), Smith and Briley (2006; M 13), and Sneden et al. (1997; M 15); the color excess  $E_{B-V}$  and the distance  $d$  (assumed to be the same for all targets in a cluster) were taken from the on-line database<sup>4</sup> elaborated by the Padova group. For  $\rho$  Boo and  $\alpha$  Boo,  $E_{B-V}$  was assumed to be zero, and the other data were taken from the SIMBAD database. We first derived  $T_{\text{eff}}$  from the dereddened  $(B - V)_0$  color by using Alonso, Arribas, and Martínez-Roger’s (1999) equation (4) in their table 2, where 0.0 ( $\rho$  Boo),  $-0.6$  ( $\alpha$  Boo),  $-1.2$  (M 4 stars),  $-1.7$  (M 13 stars), and  $-2.5$  (M 15 stars) were assumed for  $[Fe/H]$ . Then, since the stellar luminosity  $L$  can be obtained from the extinction-corrected  $V_0$  magnitude ( $V - 3.1E_{B-V}$ ), the distance  $d$ , and the bolometric correction evaluated by Alonso, Arribas, and Martínez-Roger’s (1999) equations (17) and (18), we can derive  $\log g^{\text{evo}}$  from the above-mentioned relation by assuming  $M = 0.8M_{\odot}$ . The resulting  $T_{\text{eff}}^{\text{pho}}$  and  $\log g^{\text{evo}}$  (along with the corresponding  $[Fe/H]$  values when these parameters were used; cf. table 3) are summarized in table 2, where the published values taken from various literature (since 1980’s) are also presented for comparison. Besides, table 3 gives the differences of these parameters relative to the adopted spectroscopic ones, and the resulting variations in the abundances of Fe as well as K caused by these parameter changes.

We can see the following tendency from an inspection of table 3:

- In the mildly metal-poor (M 4) or near-solar metallicity ( $\alpha$  Boo,  $\rho$  Boo) region, we can not see any remarkably systematic difference in  $\delta T_{\text{eff}} (\equiv T_{\text{eff}}^{\text{pho}} - T_{\text{eff}}^{\text{spe}})$  or in  $\delta \log g (\equiv \log g^{\text{evo}} - \log g^{\text{spe}})$ ; i.e.,  $\delta T_{\text{eff}} \sim \pm 100$  K and  $\delta \log g \sim \pm 0.2-0.3$  dex.
- However, in the very metal-poor regime of  $[Fe/H] \lesssim -1.5$  (M 13 and M 15), the inequality trend of  $\delta T_{\text{eff}} > 0$  as well as  $\delta \log g > 0$  manifestly appears, especially for the most metal-poor case of M 15 where  $T_{\text{eff}}^{\text{spe}}/\log g^{\text{spe}}$  is appre-

<sup>4</sup> (<http://dipastro.pd.astro.it/globulars/>).

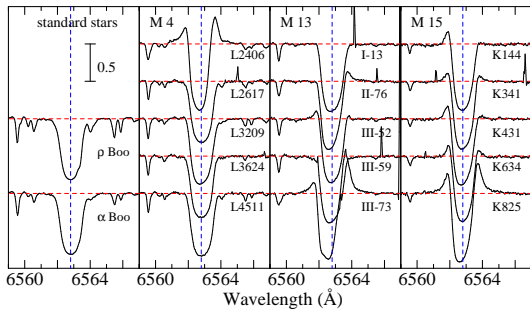


**Fig. 4.** Spectra of the 17 program stars in the 6559–6567 Å region comprising H $\alpha$ . Each spectrum is normalized with respect to the continuum (horizontally-drawn red dashed line) and is vertically shifted relative to the adjacent one by an appropriate offset (1.0 or 0.5). The wavelength scale is adjusted to the same system as in figure 3 where the stellar metallic lines locate at the laboratory wavelengths. The position of the H $\alpha$  line center (6562.8 Å) in this reference frame is indicated by the vertically-drawn blue dashed line. The redward emission for III-73 (M 13) is so strong (peaked at  $\sim 1.6$ ) that it is crossing the profile of III-59 just above.

ciably lower than  $T_{\text{eff}}^{\text{pho}}/\log g^{\text{evo}}$  by  $\sim 100\text{--}200$  K/ $\sim 1$  dex (even  $\log g^{\text{spe}} < 0$  cases are seen, which is hardly possible for hydrostatic stellar atmospheres).

Given the existence of such an appreciable discrepancy, we tend to wonder whether our use of spectroscopic parameters is really justified. Which sets ( $T_{\text{eff}}^{\text{spe}}/\log g^{\text{spe}}$  vs.  $T_{\text{eff}}^{\text{pho}}/\log g^{\text{evo}}$ ) should be preferably used for abundance determinations? Before going into this, we point out that that our targets of intrinsically bright red giants are on or near to the AGB tip where stars (in their late stage of evolution) are likely to have extended envelopes and show significant mass loss as well as time variability. Actually, as demonstrated in figure 4, not a few stars show prominent emissions and blue-shifted cores in H $\alpha$  (especially, emissions are seen in all five M 15 stars), indicating the existence of such active phenomena.

In such cases, we would state that the spectroscopic method is more advantageous:

- (1) If stars are unstable and variable in time, parameters based on observational data (colors, magnitudes, etc.) simply taken from catalogues are not reliable any more. Meanwhile, spectroscopic parameters are established from the spectrum itself, from which abundances are derived.
- (2) We must recall that most stellar model atmospheres widely used are based on the assumption of hydrostatic equilibrium and the plane-parallel approximation. In case where these assumptions failed, it would not be sensible any more to assign parameters derived from the true fundamental stellar quantities (e.g.,  $\log g^{\text{evo}}$  derived from realistic  $L$ ,  $M$ , ...). On the other hand, it is still possible to apply conventional model atmospheres, if we could choose their parameters so carefully as to reproduce the physical condition of the real atmosphere (while regarding that  $T_{\text{eff}}$  and  $\log g$  are not so much real physical quantities as rather adjustable parameters). Our  $T_{\text{eff}}^{\text{spe}}$  and  $\log g^{\text{spe}}$  should thus be interpreted in this sense.

Consequently, according to our opinion, the appreciably low  $T_{\text{eff}}^{\text{spe}}$  and low  $\log g^{\text{spe}}$  in M 13 and M 15 are nothing but a manifestation of the existence of extended cooler region of lower density affecting the formation of spectral lines. As far as we invoke classical plane-parallel model atmospheres, such low parameter values must have been assigned to reproduce the relevant atmospheric condition. Since this kind of discordance is pronounced in M 13 ( $[\text{Fe}/\text{H}] \sim -1.7$ ) and especially in M 15 ( $[\text{Fe}/\text{H}] \sim -2.5$ ) while not in M 4 ( $[\text{Fe}/\text{H}] \sim -1.1$ ), this effect is considered to be metallicity-dependent, which may presumably be related to the observational fact pointed out by Meszaros, Dupree, and Szentgyorgyi (2008) that the outflow velocities of red giants are higher in metal-poor clusters (M 15) than in metal-rich clusters (M 4). To sum up, we consider that the use of  $T_{\text{eff}}^{\text{spe}}$  and low  $\log g^{\text{spe}}$  is surely reasonable and preferable to other choices.<sup>5</sup>

## 5.2. Homogeneity of Fe and K Abundances

The results of  $[\text{Fe}/\text{H}]$ ,  $[\text{K}/\text{H}]_{7665}$ , and  $[\text{K}/\text{H}]_{7699}$  (cf. table 1) for each star are graphically depicted in figure 5, from which we can read the following characteristics:

- The  $[\text{Fe}/\text{H}]$  values are considered to be nearly uniform in all three clusters (M 4, M 13, and M 15) to within a precision of  $\sim 0.05\text{--}0.1$  dex. Actually, the mean  $\langle [\text{Fe}/\text{H}] \rangle$  (and the standard deviation  $\pm\sigma$ ) averaged over 5 stars are  $-1.14(\pm 0.04)$ ,  $-1.65(\pm 0.09)$ , and  $-2.48(\pm 0.07)$  for M 4, M 13, and M 15, respectively.<sup>6</sup> Therefore, we can state that the any of our M 4/M 13/M 15 targets have essentially the same metallicity within the cluster.
- Regarding  $[\text{K}/\text{H}]$ , for which values derived from K I 7655 and 7699 lines are consistent with each other, we notice that two stars (M 4/L2406 and M 13/III-73) are evidently anomalous because they show considerably dis-

<sup>5</sup> As an alternative interpretation, it may be possible to consider that the large discrepancy in  $\log g$  (systematically low  $\log g^{\text{spe}}$ ) seen very metal-poor red giants is due to the non-LTE overionization effect (Fe I lines are weakened compared to the case of LTE, while Fe II lines are practically unaffected), which would naturally yield an underestimation of  $\log g^{\text{spe}}$  if LTE is assumed. We can not exclude this possibility, as Ruland et al. (1980) once reported a sign of non-LTE overionization in low-excitation Fe I lines (while high-excitation lines are comparatively inert) in their analysis of the early-K giant Pollux ( $T_{\text{eff}} \sim 4800$  K,  $\log g \sim 2.2$ , and the near-solar metallicity). On the other hand, theoretical investigations on the non-LTE effect in the formation of Fe lines in red giants are difficult, because the results are sensitively influenced by uncertainties in computational details (e.g., the treatment of UV photoionizing radiation field, collisional cross section with neutral hydrogen atoms; see, e.g., Steenbock 1985 or Takeda 1991). As far as the present case is concerned, however, we consider that the possibility of an appreciable non-LTE overionization in Fe I such as claimed by Ruland et al. (1980) is rather unlikely. That is, since the characteristic feature they found was “low-excitation Fe I lines tend to yield lower LTE abundances than high-excitation Fe I lines”, the LTE excitation temperature would appear higher than usual, by which an *overestimation* of  $T_{\text{eff}}^{\text{spe}}$  should eventually result. This is, however, just the opposite to what we found in M 13 or M 15 stars.

<sup>6</sup> For reference, a simple averaging of the literature data given in table 2 (excluding our results) gives the mean cluster metallicities of  $\sim -1.2$  (M 4),  $\sim -1.5$  (M 13), and  $\sim -2.3$  (M 15).

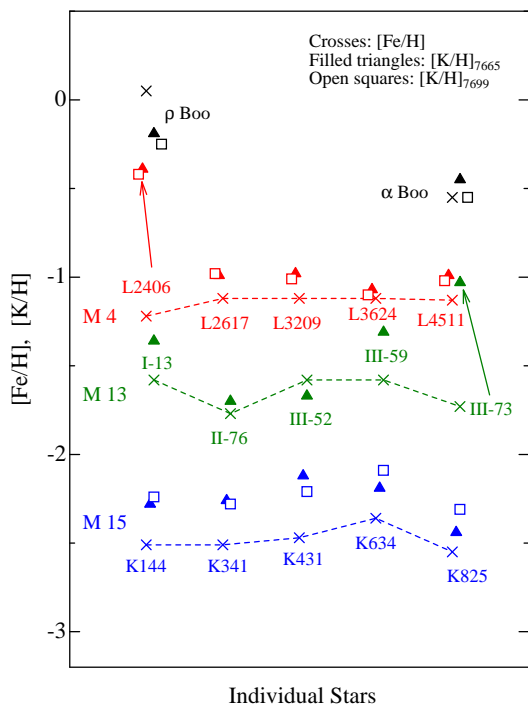


**Fig. 5.** Graphical plots of the Fe and K abundances (relative to the Sun) derived for each of the 17 stars (also given in table 1). The crosses (connected by dashed lines for those 5 stars belonging to the same cluster), filled triangles, and open squares indicate  $[\text{Fe}/\text{H}]$ ,  $[\text{K}/\text{H}]_{7665}$  (from K I 7665 line), and  $[\text{K}/\text{H}]_{7699}$  (from K I 7699), respectively. Plots for M 4, M 13, and M 15 stars are represented in red, green, and blue, respectively.

crepant (i.e., larger)  $[\text{K}/\text{H}]$  compared to other members. However, when these two stars are excluded, we can confirm a reasonable uniformity of  $[\text{K}/\text{H}]$  within a cluster; i.e.,  $\langle [\text{K}/\text{H}]_{7665} \rangle / \langle [\text{K}/\text{H}]_{7699} \rangle (\pm \sigma_{7665} / \pm \sigma_{7699})$  is  $-1.01 / -1.03 (\pm 0.04 / \pm 0.04)$  for M 4 (4 stars),  $-1.51 / -1.51 (\pm 0.20 / -)$  for M 13 (4 stars), and  $-2.26 / -2.23 (\pm 0.12 / \pm 0.09)$  for M 15 (5 stars). The larger dispersion (0.20) for the case of M 13 compared to other two clusters ( $\sim 0.05$ – $0.1$ ) may be understood as due to the availability of only one K I 7665 line which is severely contaminated by telluric lines (cf. figure 2).

How should the discrepant nature of these two outliers be interpreted? Actually, we have a good reason to believe that this is nothing but a superficial effect caused by an inadequate treatment in the abundance determination (i.e., not the real abundance anomaly). We point out that the spectra of these M 4/L2406 and M 13/III-73 have markedly broad line widths (figure 3) and prominently strong  $\text{H}\alpha$  emission components (figure 4) than the remaining stars, which suggests a significant increase in the activity or turbulent velocity fields in the upper atmosphere (where the core of K I lines form) presumably related to dynamical phenomena often seen in AGB stars. We thus suspect the existence of considerably depth-dependent turbulent velocity dispersion which in-

creases with height,<sup>7</sup> which may have contributed an additional increase to the strength of high-forming saturated K I lines. In such a case, an application of the  $v_t$  value determined from Fe lines with  $EW < 100$  mÅ would be no more adequate for the K I lines with  $EW$  of a few  $\times 100$  mÅ (especially intensified by the enhanced turbulence in the upper atmosphere), for which a somewhat larger  $v_t$  value should have been more relevant. Hence, we believe that the reason for the anomalously large  $[\text{K}/\text{H}]$  obtained for these two stars is the assignment of inappropriately small  $v_t$  values, which must have resulted in an overestimation of K abundances from such strongly saturated K I 7665/7699 lines.

Consequently, regarding that M 4/L2406 and M 13/III-73 correspond to exceptional cases of peculiar velocity fields in the upper atmospheric layer, we conclude that the abundance uniformity essentially holds for  $[\text{K}/\text{H}]$  (as well as for  $[\text{Fe}/\text{H}]$ ) within M 4, M 13, and M 15.

### 5.3. Behavior of $[\text{K}/\text{Fe}]$ over Wide Metallicities

Now that the homogeneity of K (and Fe) abundance within each globular cluster has been confirmed, we can regard based on the argument in section 1 that the observed  $[\text{K}/\text{Fe}]$  ratios (which naturally turn out also uniform) of the cluster stars retain the original composition of the halo gas, from which they formed.

According to table 1 (where the mean of  $[\text{K}/\text{Fe}]_{7665}$  and  $[\text{K}/\text{Fe}]_{7699}$  is given), the averaged cluster values of  $\langle [\text{K}/\text{Fe}] \rangle$  (and the standard deviation  $\pm \sigma$ ) are  $+0.10 (\pm 0.04)$  (M 4,  $[\text{Fe}/\text{H}] \simeq -1.1$ , 4 stars, L2406 excluded),  $+0.12 (\pm 0.16)$  (M 13,  $[\text{Fe}/\text{H}] \simeq -1.7$ , 4 stars, III-73 excluded), and  $+0.24 (\pm 0.05)$  (M 15,  $[\text{Fe}/\text{H}] \simeq -2.5$ , 5 stars). We can state from these results that  $[\text{K}/\text{Fe}]$  is marginally supersolar at  $\sim +0.1$ – $0.3$  and  $[\text{K}/\text{Fe}]$  tends to gradually increase with a decrease in the metallicity, which means a rather tight and monotonic  $[\text{K}/\text{Fe}]$  vs.  $[\text{Fe}/\text{H}]$  relation (with almost no significant diversity) in the range of  $-2.5 \lesssim [\text{Fe}/\text{H}] \lesssim -1$ . These  $[\text{K}/\text{Fe}]$  vs.  $[\text{Fe}/\text{H}]$  relations for 15 stars of M 4, M 13, and M 15 (along with  $\rho$  Boo and  $\alpha$  Boo) are plotted in figure 6, where the results for nearby F–G disk dwarfs ( $-1 \lesssim [\text{Fe}/\text{H}] \lesssim 0$ ; taken from Paper I) and those for extremely metal-poor stars ( $-4 \lesssim [\text{Fe}/\text{H}] \lesssim -2.5$ ; obtained by reanalyzing the  $EW$  data of Cayrel et al. 2004; cf. Appendix) are also shown for comparison.

As can be clearly seen from this figure, our  $[\text{K}/\text{Fe}]$  results in this study for the cluster stars (excluding M 4/L2406 and M 13/III-73) and the reference objects ( $\rho$  Boo and  $\alpha$  Boo) over  $-2.5 \lesssim [\text{Fe}/\text{H}] \lesssim 0$  connect with those of extremely metal-deficient stars as well as disk stars quite satisfactorily. We may thus conclude that  $[\text{K}/\text{Fe}]$  behaves itself in a rather clear manner over a wide  $[\text{Fe}/\text{H}]$  range of  $\sim 4$  dex from near-solar to ultra-low metallicity. That is, the gradual increase of  $[\text{K}/\text{Fe}]$

<sup>7</sup> More generally speaking, such an increasing tendency of the turbulent velocity field with height is a phenomenon occasionally seen in low-gravity stars (though its degree is different from case to case); see, e.g., Takeda (1992) for  $\alpha$  Boo (K giant) or Takeda and Takada-Hidai (1994; appendix B) for A–F supergiants.

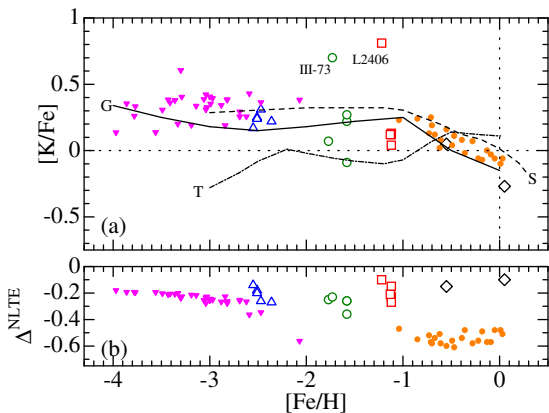


**Fig. 6.** (a) The  $[K/Fe]$  vs.  $[Fe/H]$  plots constructed from the metallicity and the NLTE potassium abundances given in table 1. The results for the 17 program stars are shown in large open symbols (diamonds for  $\rho$  Boo and  $\alpha$  Boo, squares for M 4 stars, circles for M 13 stars, and triangles for M 15 stars). The two stars (M 13 III-73 and M 4 L2406) showing exceptionally large deviations from the main trend are also indicated. Meanwhile, the smaller filled symbols represent the results for disk stars (circles, taken from Paper I) and extremely metal poor stars (inverse triangles, reanalysis of Cayrel et al.’s 2004 data, see the Appendix) presented for comparison. Lines show the three kinds of theoretical predictions (see section 1 of Paper I for more details): Dashed line (marked “S”) — Samland (1998; taken from his figure 14), dash-dotted line (marked “T”) — Timmes, Woosley, and Weaver (1995; the top curve in their figure 24), solid line (marked “G”) — Goswami and Prantzos (2000; “Case B” in their figure 7). (b) The NLTE corrections for K abundance determinations ( $\Delta^{\text{NLTE}}$  is the average of  $\Delta_{7665}^{\text{NLTE}}$  and  $\Delta_{7699}^{\text{NLTE}}$  in case that both lines are available), plotted against  $[Fe/H]$ . The same meanings of the symbols as in (a).

with a decrease in  $[Fe/H]$  ( $d[K/Fe]/d[Fe/H] \sim -0.3$ ) seen in disk stars of  $-1 \lesssim [Fe/H] \lesssim 0$  (Paper I) continues further down at  $[Fe/H] \lesssim -1$  with a slightly decreased slope until  $[Fe/H] \sim -3$ , where  $[K/Fe]$  appears to attain a broad maximum of  $\sim +0.3$  (followed by a sign of weak downturn of  $[K/Fe]$  at  $[Fe/H] \lesssim -3$ ).

Accordingly, we do not regard the considerably large diversity of  $[K/Fe]$  previously reported for halo stars of  $[Fe/H] \sim -2$  (Zhang et al. 2005, Gratton & Sneden 1987a) to be real, which we suspect to be due to some improper treatment in abundance determinations (e.g., *EW* errors caused by unsuccessful removal of telluric lines, or use of an inadequate microturbulence such as we encountered in the present cases of M 4/L2406 and M 13/III-73).

This observational fact of mildly supersolar  $[K/Fe]$  over a wide metallicity range (with  $[K/Fe] \sim 0$  at near-solar metallicity and a broad peak at  $[Fe/H] \sim -3$ ) has to be explained by theoretical calculations. However, theoreticians did not find it easy to reproduce the trend of  $[K/Fe] > 0$ , especially at the very metal-poor regime, because the K yield is metallicity-dependent (as a characteristic of odd-Z element) and becomes too small there to bring  $[K/Fe]$  above zero. Therefore, comparatively plain calculations predicted only subsolar (or near-solar

at most)  $[K/Fe]$  ratios for metal-poor stars. For example, Timmes, Woosley, and Weaver’s (1995) calculations resulted in a decrease of  $[K/Fe]$  ( $\lesssim 0$ ) with a lowering of  $[Fe/H]$  as shown figure 24 of their paper (also plotted in figure 6 as curve “T”), which markedly contradicts the observed tendency. Therefore, if the supersolar  $[K/Fe]$  is to be reenacted even at the metal-poor regime, one had to contrive ways to raise it by some means, such as empirically adjusting the K yield (Samland 1998) or using an IMF of larger exponent (cf. Goswami & Prantzos 2000; putting larger weight to comparatively less massive SNeII of lower gravitational potential), as described in section 1 of Paper I, by which a trend more or less similar to the observed one could somehow result (cf. figure 6 plotted as curves “S” and “G”, respectively). At any rate, it is evident that our understanding on the synthesis mechanism of K and its evolution in the Galaxy is still considerably insufficient (see also the Appendix for the K yield problem in the extremely metal-poor regime). Now that we have become more confident than before about the observational  $[K/Fe]$  vs.  $[Fe/H]$  trend over a wide metallicity range, we would encourage theoreticians to revisit this problem, so that a better match between theory and observation may be established in a reasonable manner.

## 6. Conclusion

Given the confusing situation regarding the  $[K/Fe]$  ratio of metal-poor stars in the halo, where some work suggests a fairly tight tendency (such like disk stars) while others report a considerably large diversity amounting to  $\sim 1$  dex, we carried out a spectroscopic study on 15 red giants of three mildly to very metal-poor globular clusters (M 4, M 13, and M 15) along with two reference stars ( $\rho$  Boo and  $\alpha$  Boo) based on the high-dispersion spectra obtained with Subaru/HDS, with a purpose of clarifying the behavior of  $[K/Fe]$  at the relevant metallicity range of  $-2.5 \lesssim [Fe/H] \lesssim -1$ .

The atmospheric parameters ( $T_{\text{eff}}$ ,  $\log g$ ,  $v_t$ , and  $[Fe/H]$ ) were spectroscopically determined by using Fe I and Fe II lines, and the abundance of K was derived from the K I resonance lines at 7664.91 and 7698.97 Å while taking into the non-LTE effect.

We confirmed that  $[K/H]$  (as well as  $[Fe/H]$ ) is almost homogeneous within each of the three clusters to a precision of  $\lesssim 0.1$  dex, though superficially large deviations are exceptionally seen for two peculiar stars which show signs of considerably increased turbulence in the upper atmosphere.

The  $[K/Fe]$  ratios of these cluster stars turned out mildly supersolar by a few tenths of dex, tending to gradually increase from  $\sim +0.1$ – $0.2$  at  $[Fe/H] \sim -1$  to  $\sim +0.3$  at  $[Fe/H] \sim -2.5$ , which is a fairly tight and clean trend. We thus consider that the previously reported large diversity of  $[K/Fe]$  in halo stars is not real, which we suspect to be due to some improper treatment in the analysis.

This result is quite consistent (i.e., smoothly connecting) with the  $[K/Fe]$  trend of disk stars ( $-1 \lesssim [Fe/H]$ ) and that of extremely metal-poor stars ( $-4 \lesssim [Fe/H] \lesssim -2.5$ ).



That is,  $[K/Fe]$  appears to continue a gradual increase from  $[Fe/H] \sim 0$  toward a lower metallicity regime down to  $[Fe/H] \sim -3$ , where a broad maximum of  $[K/Fe] \sim +0.3-0.4$  is attained, possibly followed by a slight downturn toward a further lower metallicity at  $[Fe/H] \lesssim -3$ .

This investigation is based on the data obtained by the observation with the Subaru Telescope, which was carried out during the practical training of observational astronomy for graduate students as a coursework of The Graduate University for Advanced Studies (SOKENDAI). We express our heartfelt thanks to S. S. Hayashi, R. Furuya, and A. Tajitsu for their continuous support and encouragement, as well as to C.-H. Peng and S. Honda for their collaboration in the observation.

Helpful comments by N. Tominaga and N. Iwamoto from the theoretical side on the first version of the manuscript are also acknowledged.

This research made use of the SIMBAD database operated by CDS, Strasbourg, France.

## Appendix. Reanalysis of Cayrel et al.'s (2004) Data

In the extensive spectroscopic study on the sample of 35 extremely metal-poor stars toward clarifying the abundance patterns of 17 elements from C to Zn recently carried out by Cayrel et al. (2004), the abundances of K were also determined by using K I 7665/7699 lines. However, they applied a constant non-LTE correction of  $\Delta^{NLTE} = -0.35$  dex to all stars, which they adopted as a rough estimate based on Ivanova and Shimanskiĭ's (2000) calculations. Because of this apparently imperfect treatment of the non-LTE effect, one can not be sure whether the behavior of  $[K/Fe]$  they obtained (i.e., near-solar or slightly supersolar with a decreasing tendency toward a lower metallicity from  $[K/Fe] \sim +0.2$  at  $[Fe/H] \sim -2.5$  to  $[K/Fe] \sim 0$  at  $[Fe/H] \sim -4$ ; cf. their figure 9) is reliable or not.

We decided, therefore, to reanalyze their  $EW$  data of K I 7665/7699 lines with the atmospheric parameters they used, while properly taking into account the non-LTE effect. Regarding the non-LTE departure coefficients to be included in line-formation calculations for abundance determination, we used the already calculated results for a grid of models ( $T_{\text{eff}}$  from 4500 K to 6500 K,  $\log g$  from 1.0 to 5.0,  $v_t$  from 1 to 3 km s<sup>-1</sup>, and  $[Fe/H]$  from 0.0 to -3.0), which were originally computed for constructing extensive tables of non-LTE corrections<sup>8</sup> as explained in the Appendix of Paper I. Besides, we newly performed calculations corresponding to the case of  $[Fe/H] = -4$  to be combined with the previous grids, so that we can handle any of the relevant 31 stars (for which Cayrel et

al. measured  $EW_{7665}$  and/or  $EW_{7665}$ ) in the parameter range of 4500 K  $\lesssim T_{\text{eff}} \lesssim$  5300 K,  $0.7 \lesssim \log g \lesssim 2.7$ ,  $1.2 \text{ km s}^{-1} \lesssim v_t \lesssim 2.2 \text{ km s}^{-1}$ , and  $-4.0 \lesssim [Fe/H] \lesssim -2.1$  by interpolation. Following the same manner as described in subsection 4.2, we determined  $[K/H]$ ,  $\Delta^{NLTE}$ , and  $[K/Fe]$  for each star, as given in table 4. The resulting values of  $[K/Fe]$  (as well as  $\Delta^{NLTE}$ ) are plotted against  $[Fe/H]$  in figure 6 (filled inverse triangles).

As we can see from figure 6b, the extents of the non-LTE corrections ( $|\Delta^{NLTE}|$ ) systematically decrease with a lowering of the metallicity; such as from  $\Delta^{NLTE} \simeq -0.3$  (at  $[Fe/H] \simeq -2.5$ ) to  $\Delta^{NLTE} \simeq -0.2$  (at  $[Fe/H] \simeq -4$ ), which means that Cayrel et al.'s (2004) use of  $\Delta^{NLTE} = -0.35$  must have somewhat overcorrected (i.e., underestimated)  $[K/Fe]$  by  $\sim 0.1-0.2$  dex, such that the amount of overcorrection progressively increasing with a decrease in  $[Fe/H]$ . Accordingly, regarding the  $[K/Fe]$  vs.  $[Fe/H]$  relation of extremely metal-poor stars, we consider that Cayrel et al.'s (2004) result ( $[K/Fe]$  ratio is near-solar or slightly above solar ( $\sim +0.1-0.2$ ) with an appreciable gradient of  $d[K/Fe]/d[Fe/H]$ ) should be revised as concluded in subsection 5.3 (cf. figure 6a):  $[K/Fe]$  in this very metal-deficient regime still remains well supersolar at  $\sim +0.2-0.3$ , with a marginal sign of decline (downturn) toward a further lower  $[Fe/H]$ .

The conclusion that  $[K/Fe]$  remains supersolar even at  $[Fe/H] \sim -4$  may provide theoreticians with an important constraint on the synthesis mechanism of K from the observational side, because considerable difficulties exist in theoretically reproducing the  $[K/Fe]$  ratio (cf. subsection 5.3) also in this distinctly low metallicity regime, where the observed  $[K/Fe]$  may be considered to simply reflect the composition of the first super/hyper-nova ejecta. For example, Tominaga, Umeda, and Nomoto's (2007) nucleosynthesis calculation based on population III supernova models predicted  $[K/Fe] \sim -1(\pm 0.5)$  at  $-4 \lesssim [Fe/H] \lesssim -3$  (cf. their figure 6), which apparently disagrees with the observational fact mentioned above. Hence, in order to resolve this situation, a new reassessment of assumptions or fundamental physics might as well be required. In this connection, Iwamoto et al.'s (2006) finding, that odd-Z elements such as K and Sc can be significantly overproduced if the proton-rich environment (large initial electron fraction  $Y_e$ ) is realized, is quite interesting. Further investigation following this line may be worth a try.

## References

- Alonso, A., Arribas, S., & Martínez-Roger, C. 1999, *A&AS*, 140, 261
- Anders, E., & Grevesse, N. 1989, *Geochim. Cosmochim. Acta*, 53, 197
- Bell, R. A., Edvardsson, B., & Gustafsson, B. 1985, *MNRAS*, 212, 497
- Brown, J. A., & Wallerstein, G. 1992, *AJ*, 104, 1818
- Bruls, J. H. M. J., Rutten, R. J., & Shchukina, N. G. 1992, *A&A*, 265, 237
- Carr, J. S., Sellgren, K., & Balachandran, S. C. 2000, *ApJ*, 530, 307
- Cayrel, R., et al. 2004, *A&A*, 416, 1117

<sup>8</sup> The anonymous ftp site to access these electronic tables described in the Appendix of Paper I is now not available any more. Instead, the same data materials are placed at the following web site: ([http://optik2.mtk.nao.ac.jp/~takeda/potassium\\_nonlte/](http://optik2.mtk.nao.ac.jp/~takeda/potassium_nonlte/)).

- Chen, Y. Q., Nissen, P. E., Zhao, G., Zhang, H. W., & Benoni, T. 2000, *A&AS*, 141, 491
- Cohen, J. G., & Meléndez, J. 2005, *AJ*, 129, 303
- Edvardsson, B. 1988, *A&A*, 190, 148
- Fernández-Villacañas, J. L., Rego, M., & Cornide, M. 1990, *AJ*, 99, 1961
- Gonzalez, G., & Wallerstein, G. 1998, *AJ*, 116, 765
- Goswami, A., & Prantzos, N. 2000, *A&A*, 359, 191
- Gratton, L., Gaudenzi, S., Rossi, C., & Gratton, R. G. 1982, *MNRAS*, 201, 807
- Gratton, R. G., & Ortolani, S. 1986, *A&A*, 169, 201
- Gratton, R. G., & Sneden, C. 1987a, *A&A*, 178, 179
- Gratton, R. G., & Sneden, C. 1987b, *A&AS*, 68, 193
- Hill, V. 1997, *A&A*, 324, 435
- Ivanova, D. V., & Shimanskii, V. V. 2000, *Astron. Rep.*, 44, 376
- Ivans, I. L., Sneden, C., Kraft, R. P., Suntzeff, N. B., Smith, V. V., Langer, G. E., & Fulbright, J. P. 1999, *AJ*, 118, 1273
- Iwamoto, N., Umeda, H., Nomoto, K., Tominaga, N., Thielemann, F.-K., & Hix, W. R. 2006, in *Origin of Matter and Evolution of Galaxies*, AIP Conf. Ser. 847 (American Institute of Physics), p.409
- Kraft, R. P., Sneden, C., Langer, G. E., & Prosser, C. F. 1992, *AJ*, 104, 645
- Kraft, R. P., Sneden, C., Langer, G. E., & Shetrone, M. D. 1993, *AJ*, 106, 1490
- Kurucz, R. L. 1993, Kurucz CD-ROM, No. 13 (Harvard-Smithsonian Center for Astrophysics)
- Kurucz, R. L. & Bell, B. 1995, Kurucz CD-ROM, No. 23 (Harvard-Smithsonian Center for Astrophysics)
- Kyrolainen, J., Tuominen, I., Vilhu, O., & Virtanen, H. 1986, *A&AS*, 65, 11
- Lambert, D. L., & Ries, L. M. 1981, *ApJ*, 248, 228
- Leep, E. M., Wallerstein, G., & Oke, J. B. 1987, *AJ*, 93, 338
- McWilliam, A. 1990, *ApJS*, 74, 1075
- McWilliam, A., & Rich, R. M. 1994, *ApJS*, 91, 749
- Meszaros, Sz., Dupree, A. K., & Szentgyorgyi, A. 2008, *AJ*, 135, 1117
- Noguchi, K., et al. 2002, *PASJ*, 54, 855
- Otsuki, K., Honda, S., Aoki, W., Kajino, T., & Mathews, G. J. 2006, *ApJ*, 641, L117
- Ruland, F., Holweger, H., Griffin, R., Griffin, R. F., & Biehl, D. 1980, *A&A*, 92, 70
- Samland, M. 1998, *ApJ*, 496, 155
- Shetrone, M. D. 1996, *AJ*, 112, 1517
- Smith, G. H., Shetrone, M. D., Bell, R. A., Churchill, C. W., & Briley, M. M. 1996, *AJ*, 112, 1511
- Sneden, C., Kraft, R. P., Prosser, C. F., & Langer, G. E. 1991, *AJ*, 102, 2001
- Sneden, C., Kraft, R. P., Langer, G. E., Prosser, C. F., & Shetrone, M. D. 1994, *AJ*, 107, 1773
- Sneden, C., Kraft, R. P., Shetrone, M. D., Smith, G. H., & Langer, G. E., & Prosser, C. F. 1997, *AJ*, 114, 1964
- Steenbock, W. 1985, in *Cool Stars with Excesses of Heavy Elements*, eds. M. Jaschek & P. C. Keenan (Dordrecht: Reidel), 231
- Steenbock, W. & Holweger, H. 1984, *A&A*, 130, 319
- Takeda, Y. 1991, *A&A*, 242, 455
- Takeda, Y. 1992, *A&A*, 253, 487
- Takeda, Y., Kato, K., Watanabe, Y., & Sadakane, K. 1996, *PASJ*, 48, 511
- Takeda, Y., & Takada-Hidai, M. 1994, *PASJ*, 46, 395
- Takeda, Y., Zhao, G., Chen, Y.-Q., Qiu, H.-M., & Takada-Hidai, M. 2002a, *PASJ*, 54, 275 (Paper I)
- Takeda, Y., Ohkubo, M., & Sadakane, K. 2002b, *PASJ*, 54, 451
- Takeda, Y., Ohkubo, M., Sato, B., Kambe, E., & Sadakane, K. 2005, *PASJ*, 57, 27
- Thévenin, F., & Idiart, T. P. 1999, *ApJ*, 521, 753
- Timmes, F. X., Woosley, S. E., & Weaver, T. A. 1995, *ApJS*, 98, 617
- Tominaga, N., Umeda, H., & Nomoto, K. 2007, *ApJ*, 660, 516
- Tomkin, J., & Lambert, D. L. 1999, *ApJ*, 523, 234
- Unsöld, A. 1955, *Physik der Sternatmosphären*, 2nd ed. (Berlin: Springer), 333
- Woosley, S. E., & Weaver, T. A. 1995, *ApJS*, 101, 181
- Yong, D., Lambert, D. L., Paulson, D. B., & Carney, B. W. 2008, *ApJ*, 673, 854
- Zhang, H. W., Butler, K., Gehren, T., Shi, J. R., & Zhao, G. 2006a, *A&A*, 453, 723
- Zhang, H. W., Gehren, T., Butler, K., Shi, J. R., & Zhao, G. 2006b, *A&A*, 457, 645
- Zhang, H. W., & Zhao, G. 2005, *MNRAS*, 364, 712

**Table 1.** Stellar parameters and potassium abundance results.

Star	$T_{\text{eff}}$ (K)	$\log g$ ( $\text{cm s}^{-1}$ )	$v_t$ ( $\text{km s}^{-1}$ )	[Fe/H] (dex)	$EW_{7665}$ (mÅ)	$[K/H]_{7665}$ (dex)	$\Delta_{7665}^{\text{NLTE}}$ (dex)	$EW_{7699}$ (mÅ)	$[K/H]_{7699}$ (dex)	$\Delta_{7699}^{\text{NLTE}}$ (dex)	[K/Fe] (dex)
$\rho$ Boo	4363	2.09	1.29	+0.05	*287.7	-0.19	-0.08	238.6	-0.25	-0.12	-0.27
$\alpha$ Boo	4281	1.72	1.49	-0.55	284.5	-0.45	-0.12	235.9	-0.55	-0.19	+0.05
M4 L2406	4048	0.61	2.16	-1.22	364.3	-0.39	-0.09	319.5	-0.42	-0.12	+0.81
M4 L2617	4256	1.48	1.38	-1.12	223.1	-0.99	-0.21	197.9	-0.98	-0.26	+0.13
M4 L3209	4025	1.13	1.49	-1.12	255.4	-0.98	-0.13	222.5	-1.01	-0.18	+0.12
M4 L3624	4269	1.47	1.42	-1.12	216.8	-1.07	-0.24	189.5	-1.10	-0.30	+0.04
M4 L4511	4173	1.20	1.44	-1.13	230.8	-0.99	-0.18	202.9	-1.02	-0.23	+0.12
M13 I-13	4155	0.73	1.75	-1.58	*215.4	-1.36	-0.26	...	...	...	+0.22
M13 II-76	4159	0.27	1.87	-1.77	*186.8	-1.70	-0.25	...	...	...	+0.07
M13 III-52	4271	0.80	1.55	-1.58	*168.1	-1.67	-0.36	...	...	...	-0.09
M13 III-59	4206	0.54	1.42	-1.58	*190.7	-1.31	-0.26	...	...	...	+0.27
M13 III-73	4145	0.38	1.93	-1.73	*252.8	-1.03	-0.23	...	...	...	+0.70
M15 K144	4066	-0.45	1.46	-2.51	108.2	-2.28	-0.17	90.9	-2.24	-0.18	+0.25
M15 K341	4085	-0.15	2.10	-2.51	131.2	-2.26	-0.20	102.0	-2.28	-0.19	+0.24
M15 K431	4152	-0.01	1.49	-2.47	117.8	-2.12	-0.28	89.4	-2.21	-0.25	+0.31
M15 K634	4161	0.23	1.78	-2.36	126.4	-2.19	-0.27	111.8	-2.09	-0.27	+0.22
M15 K825	4012	-0.22	1.78	-2.55	112.9	-2.44	-0.13	101.3	-2.31	-0.15	+0.17

Note.

Columns 2–5 give the atmospheric parameters (the effective temperature, the surface gravity, the microturbulence, and the Fe abundance relative to the Sun) which were spectroscopically determined by using Fe I and Fe II lines and adopted in this study. The line equivalent width, the non-LTE potassium abundance relative to the Sun, and the relevant non-LTE correction are presented in columns 6–8 (K I 7665 line) and 9–11 (K I 7699 line). In the last column 12 is given the K-to-Fe logarithmic abundance ratio, [K/Fe] ( $\equiv [K/H] - [Fe/H]$ ), where [K/H] is the average of  $[K/H]_{7665}$  and  $[K/H]_{7699}$  in case both lines are available.

\* Corrected values for the imperfect removal of telluric lines;  $\Delta EW_{\text{resid}}$  corrections of 38.8 mÅ ( $\rho$  Boo), 30.9 mÅ (I-13), 37.9 mÅ (II-76), 47.9 mÅ (III-52), 72.9 mÅ (III-59), and 22.8 mÅ (III-73) have been subtracted from the directly measured  $EW$  (cf. footnote 3 in subsection 4.1).

**Table 2.** Comparison of the atmospheric parameters and metallicity with the literature values.

Star	$T_{\text{eff}}$ (K)	$\log g$ ( $\text{cm s}^{-1}$ )	$v_t$ ( $\text{km s}^{-1}$ )	[Fe/H] (dex)	References
$\rho$ Boo	4363	2.09	1.29	+0.05	This study (adopted, spectroscopic parameters)
	4252	1.75	...	0.00	This study ( $T_{\text{eff}}^{\text{pho}}$ and $\log g^{\text{evol}}$ for reference)
	4260	2.22	2.10	-0.17	MCW90
$\alpha$ Boo	4281	1.72	1.49	-0.55	This study (adopted, spectroscopic parameters)
	4303	1.56	...	-0.65	This study ( $T_{\text{eff}}^{\text{pho}}$ and $\log g^{\text{evol}}$ for reference)
	4490	2.01	1.80	-0.56	LAM81
	4425	1.06	2.50	-0.48	GRA82
	4350	1.60	1.70	-0.58	BEL85
	4330	1.50	1.50	-0.38	GRA86
	4400	1.70	2.30	-0.55	KYR86
	4250	1.70	2.40	-0.60	LEE87
	4375	1.97	1.80	-0.42	EDV88
	4300	2.00	1.50	-0.69	FER90
	4280	2.19	2.30	-0.60	MCW90
	4330	2.10	1.60	-0.58	BRO92
	4280	1.30	1.40	-0.54	MCW94
	4300	1.50	1.70	-0.47	SNE94
	4300	1.50	1.70	-0.51	HIL97
	4250	1.30	1.70	-0.68	GON98
	4345	2.05	1.50	-0.37	THE99
	4300	1.50	1.70	-0.63	TOM99
4300	1.50	1.72	-0.49	CAR00	
M4 L2406	4048	0.61	2.16	-1.22	This study (adopted, spectroscopic parameters)
	4125	0.76	...	-1.23	This study ( $T_{\text{eff}}^{\text{pho}}$ and $\log g^{\text{evol}}$ for reference)
	4100	0.45	2.45	-1.20	IVA99
	4150	0.15	2.20	-1.30	YON08
M4 L2617	4256	1.48	1.38	-1.12	This study (adopted, spectroscopic parameters)
	4238	1.24	...	-1.21	This study ( $T_{\text{eff}}^{\text{pho}}$ and $\log g^{\text{evol}}$ for reference)
	4200	0.95	1.55	-1.17	IVA99
	4275	1.25	1.65	-1.20	YON08
M4 L3209	4025	1.13	1.49	-1.12	This study (adopted, spectroscopic parameters)
	4162	0.83	...	-1.33	This study ( $T_{\text{eff}}^{\text{pho}}$ and $\log g^{\text{evol}}$ for reference)
	3975	0.60	1.75	-1.20	IVA99
	4075	0.75	1.95	-1.25	YON08
M4 L3624	4269	1.47	1.42	-1.12	This study (adopted, spectroscopic parameters)
	4290	1.26	...	-1.22	This study ( $T_{\text{eff}}^{\text{pho}}$ and $\log g^{\text{evol}}$ for reference)
	4225	1.10	1.45	-1.16	IVA99
	4225	1.05	1.60	-1.29	YON08
M4 L4511	4173	1.20	1.44	-1.13	This study (adopted, spectroscopic parameters)
	4251	1.16	...	-1.21	This study ( $T_{\text{eff}}^{\text{pho}}$ and $\log g^{\text{evol}}$ for reference)
	4150	1.10	1.55	-1.19	IVA99
	4150	1.05	1.70	-1.22	YON08
M13 I-13	4155	0.73	1.75	-1.58	This study (adopted, spectroscopic parameters)
	4200	0.91	...	-1.57	This study ( $T_{\text{eff}}^{\text{pho}}$ and $\log g^{\text{evol}}$ for reference)
	4290	1.00	2.00	-1.46	KRA93, KRA92, SHE96
M13 II-76	4159	0.27	1.87	-1.77	This study (adopted, spectroscopic parameters)
	4212	0.91	...	-1.65	This study ( $T_{\text{eff}}^{\text{pho}}$ and $\log g^{\text{evol}}$ for reference)
	4350	1.00	2.00	-1.49	KRA93, KRA92, SHE96, SMI96
	4300	0.85	1.95	-1.53	COH05
M13 III-52	4271	0.80	1.55	-1.58	This study (adopted, spectroscopic parameters)
	4248	1.00	...	-1.56	This study ( $T_{\text{eff}}^{\text{pho}}$ and $\log g^{\text{evol}}$ for reference)
	4335	1.00	2.00	-1.50	KRA93, KRA92, SHE96
M13 III-59	4206	0.54	1.42	-1.58	This study (adopted, spectroscopic parameters)
	4260	0.97	...	-1.50	This study ( $T_{\text{eff}}^{\text{pho}}$ and $\log g^{\text{evol}}$ for reference)
	4360	1.10	1.75	-1.45	KRA93, KRA92, SHE96, SMI96
	4145	0.38	1.93	-1.73	This study (adopted, spectroscopic parameters)
M13 III-73	4177	0.81	...	-1.66	This study ( $T_{\text{eff}}^{\text{pho}}$ and $\log g^{\text{evol}}$ for reference)
	4300	0.85	2.25	-1.51	KRA93, KRA92, SHE96, SMI96
	4066	-0.45	1.46	-2.51	This study (adopted, spectroscopic parameters)
M15 K144	4242	0.74	...	-2.25	This study ( $T_{\text{eff}}^{\text{pho}}$ and $\log g^{\text{evol}}$ for reference)
	4390	0.90	2.00	-2.31	SNE91
	4460	0.95	2.00	-2.21	SNE91
	4425	0.75	2.10	-2.34	SNE97
	4085	-0.15	2.10	-2.51	This study (adopted, spectroscopic parameters)
M15 K341	4210	0.61	...	-2.35	This study ( $T_{\text{eff}}^{\text{pho}}$ and $\log g^{\text{evol}}$ for reference)
	4275	0.45	2.00	-2.34	SNE97
	4152	-0.01	1.49	-2.47	This study (adopted, spectroscopic parameters)
M15 K431	4284	0.75	...	-2.30	This study ( $T_{\text{eff}}^{\text{pho}}$ and $\log g^{\text{evol}}$ for reference)
	4430	0.90	2.00	-2.28	SNE91
	4500	1.00	2.00	-2.18	SNE91
	4375	0.50	2.30	-2.43	SNE97
	4161	0.23	1.78	-2.36	This study (adopted, spectroscopic parameters)
M15 K634	4242	0.64	...	-2.27	This study ( $T_{\text{eff}}^{\text{pho}}$ and $\log g^{\text{evol}}$ for reference)
	4225	0.30	1.85	-2.34	SNE97
	4225	0.60	2.05	-2.30	OTS06
	4012	-0.22	1.78	-2.55	This study (adopted, spectroscopic parameters)
M15 K825	4242	0.63	...	-2.30	This study ( $T_{\text{eff}}^{\text{pho}}$ and $\log g^{\text{evol}}$ for reference)
	4275	0.65	1.75	-2.42	SNE97

Note. In case that two kinds of  $\log g$  values ( $g^{\text{spe}}$  and  $g^{\text{evo}}$ ) are given for the same star (e.g., IVA99 for M 4 stars or SNE97 for M 15 stars), we preferably adopted the spectroscopic  $\log g^{\text{spe}}$ .

Key to the references: BEL85 — Bell, Edvardsson, and Gustafsson (1985); BRO92 — Brown & Wallerstein (1992); CAR00 — Carr, Sellgren, and Balachandran (2000); COH05 — Cohen & Melendez (2005); EDV88 — Edvardsson (1988); FER90 — Fernández-Villacañas, Rego, and Cornide (1990); GON98 — Gonzalez & Wallerstein (1998); GRA82 — Gratton et al. (1982); GRA86 — Gratton & Ortolani (1986); HIL97 — Hill (1997); IVA99 — Ivans et al. (1999); KRA92 — Kraft et al. (1992); KRA93 — Kraft et al. (1993); KYR86 — Kyrolainen et al. (1986); LAM81 — Lambert & Ries (1981); LEE87 — Leep, Wallerstein, and Oke (1987); MCW90 — McWilliam (1990); MCW94 — McWilliam & Rich (1994); OTS06 — Otsuki et al. (2006); SHE96 — Shetrone (1996); SMI96 — Smith et al. (1996); SNE91 — Sneden et al. (1991); SNE94 — Sneden et al. (1994); SNE97 — Sneden et al. (1997); THE99 — Thévenin & Idiart (1999); TOM99 — Tomkin & Lambert (1999); YON08 — Yong et al. (2008).

**Table 3.** Abundance variations in case that the photometric  $T_{\text{eff}}$  and the evolutionary  $\log g$  are used.

Star	$\delta T_{\text{eff}}$ (K)	$\delta \log g$ ( $\text{cm s}^{-1}$ )	$\delta[\text{Fe I}/\text{H}]$ (dex)	$\delta[\text{Fe II}/\text{H}]$ (dex)	$\delta[\text{Fe}/\text{H}]_{\text{av}}$ (dex)	$\delta[\text{K}/\text{H}]_{7665}$ (dex)	$\delta[\text{K}/\text{H}]_{7699}$ (dex)	$\delta[\text{K}/\text{H}]_{\text{av}}$ (dex)	$\delta[\text{K}/\text{Fe}]_{\text{av}}$ (dex)
$\rho$ Boo	-111	-0.34	-0.06	-0.04	-0.05	-0.05	-0.06	-0.06	0.00
$\alpha$ Boo	+22	-0.16	-0.04	-0.15	-0.10	+0.07	+0.05	+0.06	+0.16
M4 L2406	+77	+0.15	+0.03	-0.04	0.00	+0.06	+0.07	+0.06	+0.07
M4 L2617	-18	-0.24	-0.05	-0.13	-0.09	+0.03	+0.02	+0.03	+0.12
M4 L3209	+137	-0.30	-0.02	-0.40	-0.21	+0.25	+0.22	+0.24	+0.44
M4 L3624	+21	-0.21	-0.02	-0.17	-0.10	+0.07	+0.05	+0.06	+0.16
M4 L4511	+78	-0.04	+0.01	-0.17	-0.08	+0.11	+0.11	+0.11	+0.19
M13 I-13	+45	+0.18	+0.02	-0.02	0.00	+0.05	...	+0.05	+0.05
M13 II-76	+53	+0.64	+0.01	+0.23	+0.12	-0.02	...	-0.02	-0.14
M13 III-52	-23	+0.20	-0.03	+0.07	+0.02	-0.03	...	-0.03	-0.05
M13 III-59	+54	+0.43	+0.05	+0.11	+0.08	+0.03	...	+0.03	-0.05
M13 III-73	+32	+0.43	0.00	+0.15	+0.07	-0.04	...	-0.04	-0.11
M15 K144	+176	+1.19	+0.16	+0.37	+0.26	+0.08	+0.10	+0.09	-0.17
M15 K341	+125	+0.76	+0.11	+0.23	+0.17	+0.06	+0.07	+0.07	-0.10
M15 K431	+132	+0.76	+0.13	+0.22	+0.17	+0.08	+0.09	+0.09	-0.09
M15 K634	+81	+0.41	+0.10	+0.09	+0.10	+0.10	+0.11	+0.11	+0.01
M15 K825	+230	+0.85	+0.28	+0.24	+0.26	+0.20	+0.21	+0.21	-0.05

Note.

Given are the abundance variations by using the photometric  $T_{\text{eff}}$  and evolutionary  $\log g$  instead of the spectroscopically determined “standard” parameters adopted in this study (cf. table 1). (Note that the same  $EW$  data for Fe as well as K lines and the same microturbulence were used in this test calculation.) Columns 2 and 3 give the relevant changes in  $T_{\text{eff}}$  ( $T_{\text{eff}}^{\text{pho}} - T_{\text{eff}}^{\text{spe}}$ ) and  $\log g$  ( $\log g^{\text{evol}} - \log g^{\text{spe}}$ ), followed by the variation in the mean Fe abundance derived from Fe I lines (column 4), that from Fe II lines (column 5), and the average of both (column 6). Similarly, the resulting changes in the K abundances are presented in columns 7 (non-LTE K abundance from the 7665 line), 8 (non-LTE K abundance from the 7699 line), and 9 (the average of both). Finally, column 10 gives the variation in  $[\text{K}/\text{Fe}]$ , which is simply the difference in the results of columns 9 and 6.

**Table 4.** Non-LTE reanalysis of Cayrel et al.’s (2004) data.

Star	$T_{\text{eff}}$ (K)	$\log g$ ( $\text{cm s}^{-1}$ )	$v_t$ ( $\text{km s}^{-1}$ )	$[\text{Fe}/\text{H}]$ (dex)	$EW_{7665}[\text{K}/\text{H}]_{7665}$ (mÅ)	$\Delta_{7665}^{\text{NLTE}}$ (dex)	$EW_{7699}[\text{K}/\text{H}]_{7699}$ (mÅ)	$\Delta_{7699}^{\text{NLTE}}$ (dex)	$[\text{K}/\text{Fe}]$ (dex)		
HD 2796	4950	1.5	2.1	-2.47	79.8	-2.08	-0.39	49.9	-2.13	-0.30	+0.36
HD 122563	4600	1.1	2.0	-2.82	...	...	...	44.8	-2.44	-0.26	+0.38
HD 186478	4700	1.3	2.0	-2.59	93.0	-2.10	-0.43	56.0	-2.22	-0.29	+0.43
BD+17°3248	5250	1.4	1.5	-2.07	91.0	-1.67	-0.66	64.9	-1.71	-0.46	+0.38
BD-18°5550	4750	1.4	1.8	-3.06	41.5	-2.66	-0.27	24.0	-2.68	-0.24	+0.39
CD-38°245	4800	1.5	2.2	-4.19	...	...	...	...	...	...	...
BS 16467-062	5200	2.5	1.6	-3.77	5.6	-3.35	-0.20	2.0	-3.52	-0.19	+0.33
BS 16477-003	4900	1.7	1.8	-3.36	...	...	...	10.3	-2.98	-0.21	+0.38
BS 17569-049	4700	1.2	1.9	-2.88	50.0	-2.57	-0.28	35.0	-2.51	-0.26	+0.34
CS 22169-035	4700	1.2	2.2	-3.04	...	...	...	23.5	-2.73	-0.23	+0.31
CS 22172-002	4800	1.3	2.2	-3.86	5.8	-3.61	-0.19	4.8	-3.40	-0.20	+0.35
CS 22186-025	4900	1.5	2.0	-3.00	39.1	-2.59	-0.26	...	...	...	+0.41
CS 22189-009	4900	1.7	1.9	-3.49	12.5	-3.18	-0.20	...	...	...	+0.31
CS 22873-055	4550	0.7	2.2	-2.99	...	...	...	33.3	-2.64	-0.24	+0.35
CS 22873-166	4550	0.9	2.1	-2.97	...	...	...	37.5	-2.57	-0.25	+0.40
CS 22878-101	4800	1.3	2.0	-3.25	...	...	...	...	...	...	...
CS 22885-096	5050	2.6	1.8	-3.78	5.0	-3.51	-0.19	2.5	-3.53	-0.19	+0.26
CS 22891-209	4700	1.0	2.1	-3.29	30.2	-2.88	-0.23	16.7	-2.89	-0.22	+0.41
CS 22892-052	4850	1.6	1.9	-3.03	...	...	...	19.8	-2.70	-0.23	+0.33
CS 22896-154	5250	2.7	1.2	-2.69	33.1	-2.43	-0.27	22.2	-2.37	-0.25	+0.29
CS 22897-008	4900	1.7	2.0	-3.41	15.5	-3.08	-0.21	9.6	-3.02	-0.21	+0.36
CS 22948-066	5100	1.8	2.0	-3.14	...	...	...	11.2	-2.80	-0.22	+0.34
CS 22949-037	4900	1.5	1.8	-3.97	2.8	-3.86	-0.18	1.6	-3.81	-0.18	+0.14
CS 22952-015	4800	1.3	2.1	-3.43	...	...	...	10.5	-3.05	-0.21	+0.38
CS 22953-003	5100	2.3	1.7	-2.84	...	...	...	15.6	-2.65	-0.23	+0.19
CS 22956-050	4900	1.7	1.8	-3.33	...	...	...	7.4	-3.13	-0.20	+0.20
CS 22966-057	5300	2.2	1.4	-2.62	34.0	-2.38	-0.27	21.7	-2.35	-0.26	+0.26
CS 22968-014	4850	1.7	1.9	-3.56	6.7	-3.50	-0.19	5.1	-3.34	-0.20	+0.14
CS 29491-053	4700	1.3	2.0	-3.04	48.1	-2.62	-0.28	...	...	...	+0.42
CS 29502-041	4800	1.5	1.8	-2.82	52.9	-2.46	-0.29	36.1	-2.42	-0.26	+0.38
CS 29502-042	5100	2.5	1.5	-3.19	13.9	-3.00	-0.21	...	...	...	+0.19
CS 29516-024	4650	1.2	1.7	-3.06	...	...	...	...	...	...	...
CS 29518-051	5200	2.6	1.4	-2.69	30.0	-2.53	-0.25	25.0	-2.34	-0.25	+0.26
CS 30325-094	4950	2.0	1.5	-3.30	30.0	-2.69	-0.24	...	...	...	+0.61
CS 31082-001	4825	1.5	1.8	-2.91	...	...	...	...	...	...	...

Note.

The atmospheric parameters (columns 2–5) as well as the  $EW$  values for the 7665 and 7699 lines (columns 6 and 9) are from Cayrel et al. (2004). Otherwise, the meanings of the given results are the same as in table 1.